Factors Affecting Response of Cyclic Laterally Loaded Monopile in Sand

M. M. Khalaf
Future University, Cairo, Egypt

R. M. El Sherbeiny
Cairo University, Giza, Egypt

A.M. Ebid
Future University, Cairo, Egypt

S.S. Agaiby
Cairo University, Giza, Egypt

ABSTRACT: Developing a new design method for offshore monopiles has been a big challenge for several authors for decades. The challenge is proposing an accurate design methodology to account for factors affecting the cyclic response of cyclic laterally loaded monopiles, which are poorly accounted for in current guidelines such as API and DNV. These factors are sand relative density, cyclic loaded characteristics, pile geometry, pile installation method, relative pile-soil system stiffness, and grain size. Previous authors have made several attempts based on 1g and centrifuge experimental small-scale models of cyclic laterally loaded monopile to test these effects. This paper reviews most of these attempts and highlights the more affecting factors. Based on these experimental investigations, it is notable that the most damaging cyclic lateral load is an asymmetric two-way cyclic load. In addition, several empirical models developed from these experimental investigations, as well as field investigations, are concluded in this paper.

1 INTRODUCTION

Monopile foundations are extensively employed for offshore wind turbines due to their cost-effectiveness, ease of installation, and the robust supply chain supporting them. These foundations, often constructed from large steel tubes with diameters reaching up to 11 meters and aspect ratios ranging between 3 and 8, are subjected to extreme cyclic lateral loads from wind, waves, and currents in the harsh offshore environment.

Current design guidelines for monopiles, such as those provided by API and DNV, utilize the p-y curve methodology, which is based on Winkler's theory. Winkler's theory models the soil-pile interaction by treating the soil as uncoupled springs, defined nonlinearly, and the pile as an embedded beam. Reese, Cox, and Koop (1974) initially developed the p-y curves for laterally loaded piles in sand. These curves were subsequently refined by Murchison and O'Neill (1984), who demonstrated that the hyperbolic formula presented in Equation 1 yields improved results, a finding that has been adopted by the API (API RP 2A-WSD 22nd Ed. 2014).

$$p_{(x,y)} = A p_u \tanh\left(\frac{k.x}{A p_u} y\right) \tag{1}$$

$$p_u = \min of \begin{cases} (C_1.x + C_2.D)\acute{\gamma}x & \text{for } 0 < x < x_R \\ C_3.D.\grave{\gamma}.\ x & \text{for } x > x_R \end{cases} \tag{2}$$

where A is a calibration factor ($A = \left(3 - 0.8\left(\frac{x}{D}\right)\right) \geq 0.9$ for static , 0.9 for cyclic); p_u = ultimate lateral soil resistance presented in the equation; k = initial stiffness coefficient and depends on the angle of internal friction or soil relative density; C_1, C_2, and C_3 are dimensionless coefficients depending on the angle of internal friction.

The p-y curve approach utilized by API and DNV exhibits several limitations. Initially, this empirical design method was derived from field tests involving long flexible piles with an aspect ratio (L/D=34) conducted at Mustang Island. In contrast, offshore wind turbine monopiles, with aspect ratios ranging from 3 to 8, exhibit behavior akin to rigid piles, characterized by rotation rather than flexing, thereby influencing soil-pile interaction (Murchison and O'Neill, 1984). Additionally, this method modifies the static p-y curve using a factor of A=0.9 to account for cyclic loading, which incorporates the effects of accumulated rotation and variations in cyclic secant stiffness due to cyclic loading. Accurate estimation of accumulated rotation under cyclic loads is critical for the design of offshore monopiles, as the allowable rotation for wind turbine rotors is 0.5°, a parameter that governs the serviceability limit state of monopile design.

Furthermore, alterations in the cyclic secant stiffness of the pile-soil system impact the Eigen frequency of the foundation system. Consequently, predicting changes in cyclic secant stiffness due to cyclic loading is essential to prevent resonance. Cyclic load characteristics are defined by two parameters: cyclic load magnitude ratio ζ_b and cyclic load type ratio ζ_c, as provided in the equations.

$$\zeta_b = \frac{H_{max}}{H_{ult}} \tag{3}$$

$$\zeta_c = \frac{H_{min}}{H_{max}} \tag{4}$$

Where H_{max} = maximum cyclic load; H_{min} = minimum cyclic load, and H_{ult} = ultimate lateral pile capacity.

Equation [5] introduces a power law initially formulated by Little and Briaud (1988) based on full-scale investigations to predict accumulated displacement due to cyclic loading. This formulation has been corroborated by several researchers, including Peralta (2010), Klinkvort (2013), Truong et al. (2019), and Li et al. (2022). Results from 1g experimental tests indicate that the power law aptly describes the long-term cyclic response of rigid piles, whereas the logarithmic formula, as presented in equation [6], better fits the long-term cyclic response of flexible piles (Peralta, 2010). Furthermore, Little and Briaud (1988) observed an exponential degradation of the secant stiffness in the soil-pile system with load cycles, as shown in equation [7]. Contrarily, an exponential increase in cyclic secant stiffness with the number of cycles was reported by Li et al. (2022).

$$y_N = y_1 . N^a \tag{5}$$

$$y_N = y_1 . (1 + t \ln N) \tag{6}$$

$$K_{s,N} = K_{s,1} . N^\beta \tag{7}$$

where a, t, and β = cyclic accumulation parameters.

LeBlanc, Houlsby, and Byrne (2010) proposed an alternative power formula, detailed in equation [8], derived from a series of 1g experimental tests. This formula was subsequently validated by multiple researchers, including Nicolai and Ibsen (2014), Albiker et al. (2017), Frick and Achmus (2020), and Richards, Byrne, and Houlsby (2020), who observed a good fit with the cyclic response of model piles. Furthermore, it was observed that the cyclic secant stiffness increases logarithmically with the number of cycles, as presented in equation [9] (LeBlanc, Houlsby, and Byrne 2010; Klinkvort 2013; Nicolai and Ibsen 2014).

$$\frac{\Delta\theta}{\theta_S} = T_b . T_c . N^\alpha \tag{8}$$

$$\tilde{k} = \tilde{k}_0 + A_k \ln(N) \tag{9}$$

where T_b and T_c= nondimensional constants; α= cyclic accumulation coefficient; $\tilde{k}_0$= normalized initial stiffness, A_k = nondimensional coefficient. **Table 1** summarizes some of the developed empirical models based on 1g, centrifuge, and field tests to estimate field tests to estimate the cyclic response of offshore monopiles. All piles used are rigid to mimic offshore wind turbines monopile foundation systems.

Table 1 Cyclic Monopile Response Models Based on 1g, Centrifuge, and Field Tests.

Authors	Test type	Model	Parameters
Leblanc et al. (2010)	1g	$\frac{\Delta\theta}{\theta_S} = T_b(\zeta_b, D_r).T_c(\zeta_c).N^{\alpha}$	$T_b(\zeta_b, Dr = 0.04) = 0.414\zeta_b - 0.023$ $T_b(\zeta_b, Dr = 0.38) = 0.414\zeta_b - 0.023$ $T_c(\zeta_c) = * a\zeta_c^4 + * b\zeta_c^3 + * c\zeta_c^2 + d\zeta_c + * e$ $\alpha = 0.31$
Peralta (2010)	1g	Rigid pile: $y_N = y_1.N^m$ Flexible pile: $y_N = y_1.(1 + t\ln N)$	m =0.12, t = 0.21
Klinkvort et al. (2013)	25g, 75g	$\tilde{y}_{max,N} = \tilde{y}_{max,1} \times N^{\alpha}$	$\alpha(\zeta_b, \zeta_c) = T_c(\zeta_c).T_b(\zeta_b)$ $T_b(\zeta_b) = 0.61\zeta_b - 0.013$ $T_c(\zeta_c) = (\zeta_c + 0.63)(\zeta_c - 1)(\zeta_c - 1.64)$
Li et at (2015)	field	$y_N = y_1.N^a$	a= 0.085, b= 0.125
Truong et al. (2018)	60g, 250g	$y_N = y_1.N^{\alpha_Y}$	$\alpha_y = (0.3 - 0.22D_r)[1.2(1 - \zeta_c^2)(1 - 0.3\zeta_c)]$
Li et al (2020)	100g	$\frac{y_{max,N}}{Y_{max,a}} = N^{\alpha(\zeta_b,\zeta_c)}$	$\alpha(\zeta_b, \zeta_c) = T_c(\zeta_c).T_b(\zeta_b)$ $T(\zeta_b) = 0.0733$ $T_c(\zeta_c) = -1.707(\zeta_c + 0.31)^2 + 0.949$, $D_r = 80\%$ $T_c(\zeta_c) = -1.14(\zeta_c + 0.323)^2 + 1.263$ $D_r = 50\%$
Frick and Achmus (2022)	1g	$y_N = y_1.N^{\alpha(\zeta_c)}$	$\alpha(\zeta_c) = 0.0958 - 0.0858\zeta_c - 0.1576\zeta_c^2 + 0.1476\zeta_c^3, ** LB$ $\alpha(\zeta_c) = 0.14 - 0.1466\zeta_c - 0.1176\zeta_c^2 + 0.1238\zeta_c^3, ** UB$

*Polynomial coefficients of: T_c ($\zeta_c \leq$ -0.3): a= 113.33; b= 288.5; c= 238.88; d= 73.48; e= 9.94 & Tc ($\zeta_c >$ -0.3): a= 3.06; b= -6.5; c= 5.22; d= -2.76; e= 0.99

** LB means the lower boundary of accumulation coefficient $\alpha(\zeta_c)$; UB means the upper boundary of accumulation coefficient $\alpha(\zeta_c)$

2 COMPARATIVE STUDY

A comparative analysis has been conducted among various empirical models to identify the common factors influencing the cyclic lateral response of monopiles. The study utilized a pile with a diameter of 10 m and a wall thickness of 0.1 m, with varying parameters detailed in Table 2. In this parametric study, the absolute values of the maximum cyclic load (H_{max}) were considered instead of the maximum cyclic load ratio (ζ_b) due to the challenges in determining the ultimate lateral pile capacity and the differing failure criteria assumed in the referenced empirical models. These criteria are listed in Table 3. The formulation developed by LeBlanc, Houlsby, and Byrne (2010) estimates accumulated displacement rather than accumulated rotation. The monotonic response of the monopile is characterized by the PISA model, which utilizes modified p-y curves developed by an academic group led by Oxford University. This model is integrated into the PLAXIS Monopile Designer software, which calculates the monotonic displacement at the mudline (y1) corresponding to each maximum cyclic load and determines the pile monotonic capacity (Hult) according to the failure criteria adopted by the mentioned authors. The sand index and strength parameters used in the PLAXIS Monopile design are based on the sand relative density according to Brinkgreve and Engin (2010), as specified in Table 4. Figure 1 illustrates the monopile's monotonic response with a diameter of 10 m, a wall thickness of 0.1 m, an aspect ratio (L/D), normalized load eccentricity (h/L), flexural stiffness (EI) of 8×10^9 kN·m², and a sand relative density of 0.75. The figure also provides the monotonic pile capacity corresponding to

each failure criterion. The accumulated lateral deflection due to cyclic loading was determined using the various empirical models listed in Table 1.

Table 2 Range of Parametric Study

Sand relative density (Dr) %	50	55	60	65	70	75		
Pile aspect ratio (L/D)	3	4	5	6				
Normalized Load eccentricity (h/L)	0.6	0.8	1	1.2				
Maximum cyclic load (H_{max}) (MN)	5	7	9	11	13	15	17	19
Cyclic load type ratio (ζ_c) (-)	0.25	0	-0.25	-0. 5	-0.75	-1		

Table 3 Failure Criteria Adopted by the Mentioned Authors

Author	Failure criteria	H_{ult} (kN) Dr = 0.75, D/L = 4, h/L =1
Peralta et al. (2010)	*y_{mud} = 0.1 L	42239.397
LeBlanc, Houlsby, and Byrne (2010)	$\widetilde{\theta} = \theta_{ref}.\sqrt{\frac{p_a}{L.\dot{\gamma}}} = 4°$	40959.52
linkvort et al. (2013)	θ = 4°	35530.425
Li et at (2015)	y_{mud} = 0.05D	22358.109
Truong et al. (2018)	θ = 0.5°	12442.066
Li et al (2020)	y_{mud} = 0.075D	27242.966
Frick and Achmus (2022)	Hyperbolic formula (Manolui et al. 1985)	45937.411

*y_{mud} means lateral pile displacement at the sand surface.

Table 4 Sand parameters used in PLAXIS monopile designer according to Brinkgreve and Engin (2010)

Parameter	Correlation
Sand-saturated unit weight (γ_{sat}) kN/m^3	$\gamma_{sat} = 19 + 1.69\ D_r/100$
Reference initial shear modulus (G_o^{ref}) kN/m^2	$G_o^{ref} = 60000 + 68000 D_r/100$
Effective angle of internal friction ($\dot{\varphi}$) °	$\dot{\varphi} = 28 + 12.5\ D_r/100$
Angle of dilatancy (ψ) °	$\psi = \dot{\varphi} - 30$
At rest earth pressure coefficient (k_o)	$k_o = 1 - \sin\dot{\varphi}$

3 FACTORS AFFECTING THE CYCLIC RESPONSE OF MONOPILE

3.1 *Sand relative density*

As depicted in Figure 2, all authors have reported that the pile accumulated displacement (y_N/y_1) exhibits an exponential increase with the number of load cycles. Under one-way cyclic loading conditions (ζ_c=0), the accumulated displacement is minimally influenced by the relative density of sand, a factor that can generally be disregarded. However, Truong et al. (2019) observed a significant reduction in accumulated displacement with increasing relative density, attributing this to the accumulation coefficient (α) being dependent on sand relative density. In the case of two-way cyclic loading, the pile accumulated displacement is affected by sand relative density, though additional experimental studies are required to substantiate and quantify this effect. Conversely, the relative density of sand predominantly affects the pile static displacement (y_1). Figure 2

illustrates the impact of load cycle number and relative density on pile accumulated displacement. It is noteworthy that the models proposed by Peralta et al. (2010) and Frick and Achmus (2022) yield nearly identical accumulated displacement values under one-way cyclic loading conditions.

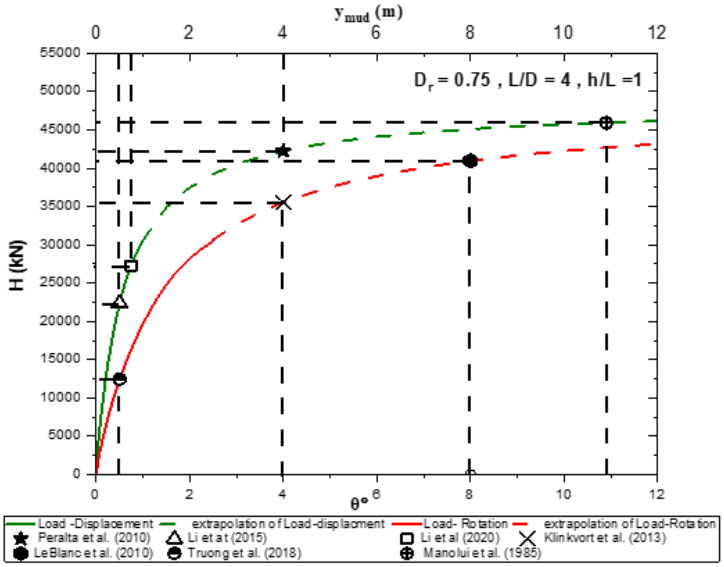

Figure 1. Monotonic load -displacement and rotation curves with failure criteria.

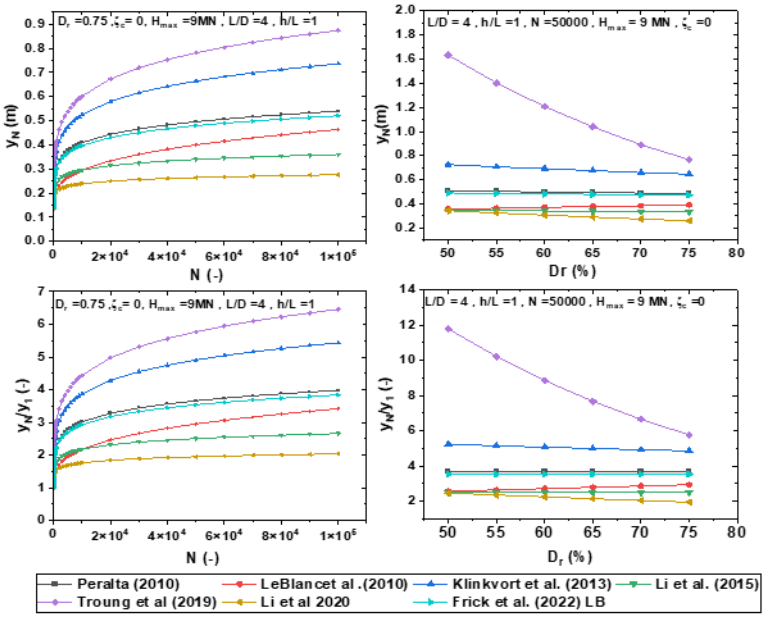

Figure 2. Effects of number of cycles and sand relative density.

3.2 *Cyclic load characteristics (ζ_b, ζ_c)*

Empirical models generally indicate that under one-way cyclic loading (ζ_c = 0), the pile accumulated displacement (y_N/y_1) is independent of the cyclic load magnitude, with the exception of Klinkvort (2013). Klinkvort's centrifuge test results demonstrated that the pile accumulated displacement (y_N/y_1) significantly increases with cyclic load magnitude (H_{max}). This increase is attributed to the accumulation coefficient (α), which is influenced by the nondimensional parameter $T_{b,K}$, itself increasing linearly with the cyclic load magnitude ratio (ζ_b). Similarly, LeBlanc, Houlsby, and Byrne (2010) observed that pile accumulated displacement is affected by cyclic load magnitude, increasing with H_{max}, due to the nondimensional parameter Tb,LeB being linearly proportional to ζ_b. Moreover, the cyclic load magnitude ratio (ζ_b) primarily affects pile static displacement (y1).

As illustrated in Figure 3, pile accumulated displacement (y_N/y_1) is highly sensitive to the type of cyclic load. Most developed models indicate that the largest accumulated displacement occurs under asymmetric two-way cyclic loading, with cyclic load type ratio (ζ_c) ranging between -0.2 and -0.6, except for Klinkvort (2013), who observed that the maximum displacement occurs under one-way cyclic loading. The empirical models by Peralta et al. (2010) and Li et al. (2015) do not account for the effect of cyclic load type. This conclusion is supported by particle image velocimetry (PIV), which attributes the minimal net soil compaction around the pile during asymmetric two-way cyclic loading as the primary reason. Additionally, transitioning from one-way to two-way cyclic loading increases the cyclic secant stiffness accumulation rate (Frick and Achmus, 2020; Li et al., 2022).

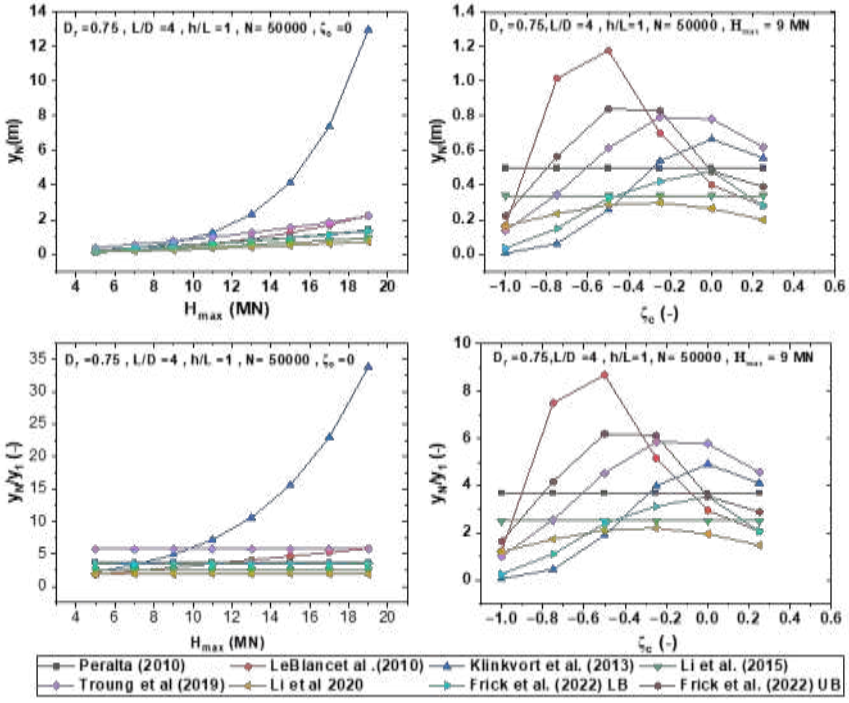

Figure 3. Effects of cyclic load magnitude (H_{max}) and cyclic load type ratio (ζ_c).

3.3 *Pile Geometry and load eccentricity effects (L/D, h/L)*

Most previous empirical models, derived from 1g centrifuge tests of rigid piles, indicate that under one-way cyclic loading, the accumulated displacement of the pile (y_N/y_1) is independent of the pile aspect ratio (L/D), as depicted in Figure 4. Conversely, the models developed by LeBlanc, Houlsby, and Byrne (2010) and Klinkvort (2013) demonstrate that the accumulated displacement of the pile significantly decreases with an increase in the pile aspect ratio (L/D). This discrepancy arises because these models are proportional to the cyclic load magnitude ratio (ζ_b), which decreases as the ultimate pile lateral capacity (H_{ult}) increases with the pile aspect ratio (L/D). Figure 5 illustrates that all empirical models, except those proposed by LeBlanc, Houlsby, and Byrne (2010) and Klinkvort (2013), confirm the independence of pile accumulated displacement from the cyclic load eccentricity (h/L). However, the latter models show an increase in pile accumulated displacement with increasing cyclic load eccentricity, as they are proportional to the cyclic load magnitude ratio, which rises with cyclic load eccentricity due to the inverse relationship with ultimate lateral pile capacity. For two-way cyclic loading, Frick and Achmus (2022) found that both the pile aspect ratio (L/D) and cyclic load eccentricity influence the accumulated displacement of the pile. Nonetheless, further investigation is required to quantify these effects.

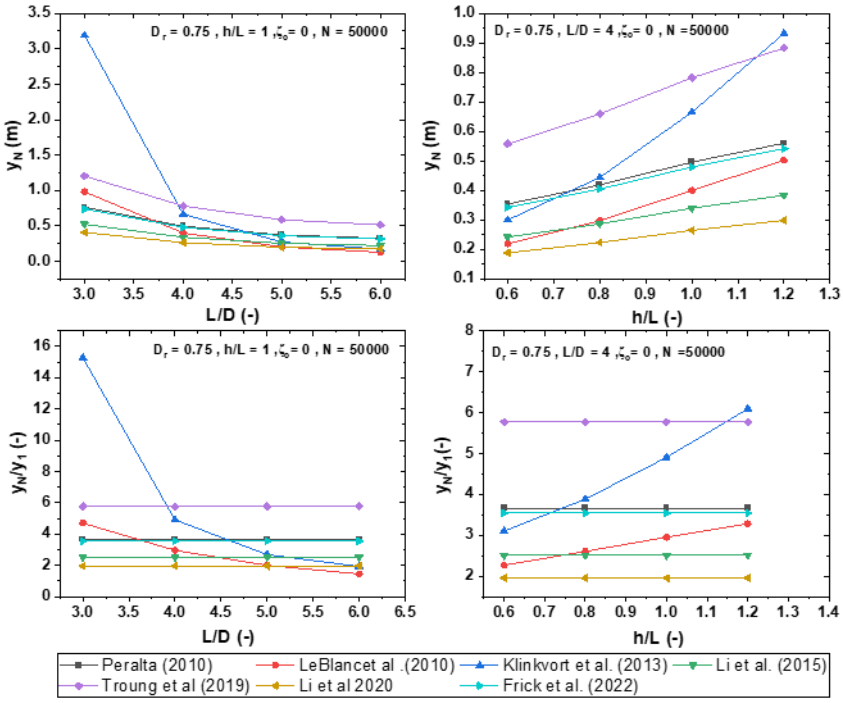

Figure 4. Effects of pile aspect ratio (L/D) and the cyclic load eccentricity (h/L)

3.4 *Pile installation method effects*

According to the centrifuge tests conducted by Fan, Bienen, and Randolph (2021), the ultimate capacity and initial stiffness of monopiles subjected to cyclic lateral loading in medium-dense sand are significantly influenced by the pile installation method. The results indicated that impact-driven piles exhibit greater ultimate capacity and initial stiffness compared to jacked piles. This variance is attributed to changes in the soil state induced by the installation method, which subsequently affects the Eigen frequency of offshore wind turbines and, in turn, influences their fatigue limit state design.

Bienen et al. (2021) utilized Abaqus/CEL to simulate the large-deformation event during pile installation. The installation results were then transferred to Abaqus/Standard through a MATLAB routine to incorporate the effects of the installation process into the lateral loading model. This numerical modelling demonstrated that the pile installation method significantly alters the surrounding soil state (void ratio, horizontal stresses), corroborating the findings of Fan, Bienen, and Randolph (2021). The study confirmed that impact-driven piles have greater capacity and initial stiffness compared to jacked and wished-in-place piles.

4 CONCLUSION

Based on the results of the comparative study, it was determined that the cyclic load type ratio (ζ_c) exerts a significant influence on the accumulation rate of lateral displacement in piles subjected to cyclic loading. Conversely, parameters such as sand relative density, pile geometry, lateral load eccentricity, and cyclic load magnitude were found to have minimal impact on lateral displacement accumulation in monopiles under single-cycle loading conditions. These parameters appear to affect accumulated pile displacement under two-cycle loading conditions, though further investigation is necessary to substantiate these findings. Previous centrifuge tests and numerical modelling of substantial deformation events during installation have demonstrated that the method of pile installation markedly alters the state of the surrounding soil (e.g., void ratio and horizontal stresses), thereby influencing monopile response. Furthermore, observations

indicate that impact-driven piles exhibit greater pile capacity and initial stiffness compared to jacked and wish-in-place piles.

REFERENCES

Albiker, J., Achmus, M., Frick, D., & Flindt, F. (2017). 1 g model tests on the displacement accumulation of large-diameter piles under cyclic lateral loading. *Geotechnical Testing Journal*, *40*(2), 173-184.

API RP 2A-WSD 22nd Ed. 2014. "*Planning, Designing, and Constructing Fixed Offshore Platforms - Working Stress Design*." API Recommended Practice (November 2014): 324.

Bienen, B., Fan, S., Schröder, M., & Randolph, M. F. (2021). Effect of the installation process on monopile lateral response. *Proceedings of the Institution of Civil Engineers-Geotechnical Engineering*, *174*(5), 530-548.

Brinkgreve, R.B.J., Engin, E., & Engin, H.K. (2010). Validation of empirical formulas to derive model parameters for sands. *Numerical methods in geotechnical engineering*, *1*, 137-142.

Byrne, B. W., McAdam, R., Burd, H. J., Houlsby, G. T., Martin, C. M., Zdravkovic, L., ... & Skov Gretlund, J. (2015). New design methods for large diameter piles under lateral loading for offshore wind applications. *Frontiers in offshore geotechnics III*, 705-710.

Fan, S., Bienen, B., & Randolph, M. F. (2021). Centrifuge study on effect of installation method on lateral response of monopiles in sand. *International Journal of Physical Modelling in Geotechnics*, *21*(1), 40-52.

Frick, D., & Achmus, M. (2020). An experimental study on the parameters affecting the cyclic lateral response of monopiles for offshore wind turbines in sand. *Soils and Foundations*, *60*(6), 1570-1587.

Frick, D. & Achmus, M. (2022) A Model Test Study on the Parameters Affecting the Cyclic Lateral Response of Monopile Foundations for Offshore Wind Turbines Embedded in Non-Cohesive Soils. *Wind Energy Science,* 7(4): 1399–1419.

Klinkvort, R. T., & Hededal, O. (2013). Lateral response of monopile supporting an offshore wind turbine. *Proceedings of the Institution of Civil Engineers-Geotechnical Engineering*, *166*(2), 147-158.

LeBlanc, C., Houlsby, G. T., & Byrne, B. W. (2010). Response of stiff piles in sand to long-term cyclic lateral loading. *Géotechnique*, *60*(2), 79-90.

Li, Q., Askarinejad, A., & Gavin, K. (2022). Lateral response of rigid monopiles subjected to cyclic loading: centrifuge modelling. *Proceedings of the Institution of Civil Engineers-Geotechnical Engineering*, *175*(4), 426-438.

Li, W., Igoe, D., & Gavin, K. (2015). Field tests to investigate the cyclic response of monopiles in sand. *Proceedings of the Institution of Civil Engineers-Geotechnical Engineering*, *168*(5), 407-421.

Little, R. L., & Briaud, J. L. (1988). *Full-scale cyclic lateral load tests on six single piles in sand*. US Army Engineer Waterways Experiment Station, Geotechnical Laboratory.

Murchison, J. M., & O'Neill, M. W. (1984, October). Evaluation of py relationships in cohesionless soils. In *Analysis and design of pile foundations* (pp. 174-191). ASCE.

Nicolai, G., & Ibsen, L. B. (2014). Small-scale testing of cyclic laterally loaded monopiles in dense saturated sand. In *ISOPE International Ocean and Polar Engineering Conference* (pp. ISOPE-I). ISOPE.

Peralta, Peter. 2010. "*Investigations on the Behavior of Large Diameter Piles under Long-Term Lateral Cyclic Loading in Cohesionless Soil*."

Reese, L.C., Cox, W.R., & Koop, F.D. (1974). "Analysis of Laterally Loaded Piles in Sand." *In Proceedings of the Annual Offshore Technology Conference, Offshore Technology Conference*, 473–80.

Richards, I.A., Byron, B.W., and Houlsby, G.T. (2020). Monopile Rotation under Complex Cyclic Lateral Loading in Sand. *Geotechnique*, 70(10): 916–930.

Truong, P., Lehane, B.M., Zania, V., and Klinkvort, R.T. (2019). Empirical Approach Based on Centrifuge Testing for Cyclic Deformations of Laterally Loaded Piles in Sand. *Geotechnique*, 69(2): 133–145.